

# Processing and Characterization of AA2024/Al<sub>2</sub>O<sub>3</sub>/SiC Reinforced Hybrid Composites Using Squeeze Casting Technique

M. Senthil Kumar<sup>1\*</sup>, R. V. Mangalaraja<sup>2</sup>, R. Senthil Kumar<sup>3</sup> and L. Natrayan<sup>1</sup>

\*msv305@yahoo.co.in

Received: May 2018

Revised: August 2018

Accepted: September 2018

<sup>1</sup> School of Mechanical and Building Sciences, VIT, Chennai, India.

<sup>2</sup> Department of Materials Engineering, Faculty of Engineering, University of Concepcion, Concepcion, Chile.

<sup>3</sup> Department of Mechanical Engineering, Dhaanish Ahmed College of Engineering, Chennai, India.

DOI: 10.22068/ijmse.16.2.55

**Abstract:** The present requirement of the automobile industry is seeking lightweight material that satisfies the technical and technological requirements with better mechanical and tribological characteristics. Aluminum matrix composite (AMC) materials meet the requirements of modern demands. AMCs are used in automotive applications as engine cylinders, pistons, disc, and drum brakes. This paper investigates the effect of particle size and wt% of Al<sub>2</sub>O<sub>3</sub>/SiC reinforcement on mechanical and tribological properties of hybrid metal matrix composites (HMMCs). AA2024 aluminum alloy is reinforced with Al<sub>2</sub>O<sub>3</sub>/SiC different particle sizes (10, 20 and 40 μm) and weight fractions (upto 10 wt %) fabricated by using a squeeze casting technique. HMMCs were characterized for its properties such as X-ray diffraction (XRD), density, scanning electron microscope (SEM), hardness, tensile strength, wear and coefficient of friction. AA2024/5wt%Al<sub>2</sub>O<sub>3</sub>/5wt%SiC with 10 μm reinforced particle size showed maximum hardness and tensile strength of 156.4 HV and 531.43 MPa and a decrease in wear rate was observed from 0.00307 to 0.00221 at 10N. Hybrid composites showed improved mechanical and wear resistance suitable for engine cylinder liner applications.

**Keywords:** Hardness, Density, Tensile strength, Wear, Squeeze casting and Particle size.

## 1. INTRODUCTION

The current requirement of automotive industries is to seek improved fuel efficiency, properties, friction and wear resistance [1]. This led to the development of lightweight and low-cost material for cylinders block, liners, piston, cam-shafts, lifters, brake components, frame members, etc [2]. The cylinder liner serves as a sliding surface for the piston rings retaining the lubricant. The combustion heat taken up by the piston and piston rings transmits to the coolant. Failure of the liners can affect the performance of the engine seriously. This leads to mechanical energy loss and emits a significant amount of particulate emissions. Cast iron (CI) cylinder liners offer excellent wear-resistance at high temperatures. The limitation of the CI liner is the development of air pockets that lead to premature failure of an engine cylinder. To overcome this limitation, metal matrix composite (MMC) were used as cylinder liners with superior tribological characteristics and sufficient strength. Selection of right material for an engineering application depends on properties such as

strength, wear, density, light-weight, melting point, cost, etc. Though, aluminum (Al) and mild steel showed better response compared to other materials. Steel whose density is three times of Al, with low coefficient of thermal expansion (CTE) and thermal conductivity makes it an unlikely material for cylinder liners. Al stands out as a better choice due to its good thermal conductivity. Moreover, CTE found to be similar to Al piston and it satisfies the requirement of low weight. Al and its alloys show low hardness and degradation in mechanical and tribological properties at elevated temperatures, which limits its application in engineering [3-5].

It is well known, that the addition of reinforcement (hard material) to the matrix (Metal matrix composites-MMC) improves the mechanical and tribological properties [6, 7]. MMCs retain the property of toughness and ductility derived from matrix, strength, and stiffness from the reinforcement. Tailoring the mechanical properties of MMC for a specific application is identified by matrix, type, size and amount of reinforcement, and the fabrication technique.

Matrix materials used in MMCs are Al, Mg, Gr, Ti, etc. Though, Ti, Mg, and Al are popular matrix materials. Ti known for its high specific strength has a density twice the Al and is reactive at high temperatures. While Mg and its alloys possess good specific mechanical properties, its low absolute strength and limited ductility limit the application. Al and its alloys showed a better response as a matrix material [8] due to its low density, high thermal conductivity and potentially a stable material for tribological applications. Addition of impurities in Al alloys exhibit a heterogeneous microstructure. It is seen apparently in high strength Al alloys 2xxx, 6xxx, 7xxx and 8xxx series. The selection of an Al alloy is totally based on a specific engineering application. AA2xxx series satisfies the requirement of high strength for aerospace and automotive applications. It shows better mechanical properties and low wear resistance [9].

Similarly, the proper selection of reinforcement helps the AMC in achieving the desired mechanical properties [10].  $\text{Al}_2\text{O}_3$ , SiC, Gr,  $\text{B}_4\text{C}$ ,  $\text{Si}_3\text{N}_4$ , TiC,  $\text{TiB}_2$ ,  $\text{TiO}_2$ , Ti and W [11-13] are the reinforcement used. The most commonly used reinforcements are  $\text{Al}_2\text{O}_3$  and SiC. The reinforcement  $\text{Al}_2\text{O}_3$  offered good wear resistance and the tensile strength, hardness, density and wear resistance increase with SiC addition to Al and its alloys [14]. Increase in the volume fraction of  $\text{Al}_2\text{O}_3$  (15 Vol%) in Al2024, increased the ultimate tensile strength [15] and decreased the ductility [16]. The application of pressure in molten Al decreases the porosity and improves wettability and bonding in AA2024/ $\text{Al}_2\text{O}_3$  composite [17]. Al2024 composite fabricated with different particle sizes (16, 32, 66  $\mu\text{m}$ ) of  $\text{Al}_2\text{O}_3$  reinforcement increase the composite hardness and tensile strength with increase in  $\text{Al}_2\text{O}_3$  volume fraction up to 10 % at the lowest particle size (16  $\mu\text{m}$ ). Wear resistance of composites decreased with increasing sliding distance, abrasive grit size and load [18]. The wear behavior is affected by the size of the particulates. Steady load on composites with large particulate size displayed exceptional wear resistance [19]. SiC (15 wt%) reinforced AMC demonstrate good strength, hardness and wear resistance [20]. The ultimate tensile strength, yield strength, hardness and compressive strength of Al2024/SiC/Gr hybrid composite increase with an increasing volume fraction of reinforcement [21]. The wear rate of AMC reinforced SiC increased by increasing the load, speed and sliding distances [22].

AMCs offer better strength at high temperatures, good wear resistance, stiffness, low coefficient of friction and thermal expansion [23,24]. The hardness of composites increased with increase in wt% of the reinforcement [25]. The particulates  $\text{Al}_2\text{O}_3$  and SiC offers good support in tailoring the properties for its application in aerospace, automobiles and various other fields [26].

Selection of right fabrication technique for the processing of HMMC improves the mechanical properties. So, far no unique processing route has been identified in particular. Different fabrication techniques in practice are liquid metal infiltration [27] stir-casting [28-30], squeeze casting [31], etc. Traditional stir casting process reported segregation, micro-porosity and poor adhesive nature of the composites [14,32]. The novel squeeze casting technique has the potential to overcome these limitations. Its advantage is cast components can be fabricated in a single step process with low squeeze pressure. Hence, along with the low cost of starting materials makes squeeze casting a preferable method for manufacturing of components. Thermal limitations of the die restrict the squeeze casting to light and low melting point alloys of aluminum and magnesium. The squeezing pressure shows the effect of undercooling along with the dissipation of heat through the dies that promote quick solidification. It reduces the contact time between the reinforced particles and the molten aluminum and decreased the possibility of interfacial reactions [33]. The squeezing pressure of 100 MPa and time duration of 30 sec [34] is found to be adequate to obtain microstructural refinement, reduction in porosity, and achieve a complete contact between the metal and the die surface.

This makes it suitable for the manufacture of light alloy components in large production quantities. Higher solidification rate helps in reinforcement distribution, decrease in porosity, low operating costs and good surface finish [35] exhibiting better mechanical properties. Hence, it stands out as an attractive processing technique [36].

The drive-by automotive industries towards sustainable growth and contribution towards society's life improvement greatly depends on the use of alternative materials made them use the MMCs extensively. The requirement of good mechanical properties and wear resistance necessitated the need for hybrid metal matrix composites (HMMC) combin-

ing the advantages of reinforcement. This made the research to be conducted remarkably by using the  $\text{Al}_2\text{O}_3$  and SiC reinforced with AA2024 to study its suitability for liner application. This paper attempts, the fabrication of HMMC using reinforcement  $\text{Al}_2\text{O}_3/\text{SiC}$  with different wt% (1-10 wt%) and particle sizes (10, 20 and 40  $\mu\text{m}$ ) using a squeeze casting technique. The prepared samples were characterized to understand the properties such as density, XRD, tensile, hardness, wear, coefficient of friction and wear microstructure.

## 2. EXPERIMENTAL PROCEDURE

Fig. 1 shows the setup of the squeeze casting process used in the fabrication of HMMCs. AA2024 alloy was chosen as a metal matrix and reinforcement with different wt% of  $\text{Al}_2\text{O}_3$  (Sigma Aldrich, 99.9%) and SiC (Sigma Aldrich, 97.5%) was used. The composition of the matrix and reinforcement selected is shown in table 1.

**Table 1.** The composition of HMMC in wt%

Sample Code	(AA2024)	$\text{Al}_2\text{O}_3$	SiC
S1	99	0.5	0.5
S2	98	1	1
S3	96	2	2
S4	94	3	3
S5	92	4	4
S6	90	5	5

In order to study the effect of reinforcements,  $\text{Al}_2\text{O}_3$  and SiC particulates were milled to obtain 10, 20 and 40  $\mu\text{m}$  particle sizes, respectively. Based on the composition, appropriate wt% of AA2024 alloy was taken in the graphite crucible and heated in the furnace at 750 °C. Mg 1 wt% was added into the molten alloy to increase the wettability of the reinforcements into the matrix. Die consists of two stainless steel spacers, die, base and stainless steel plunger. The cylindrical shaped die is considered to minimize leakage, deliver constant pressure and ensure even ejection of the cast. The dimensions of the die cavity are 250 mm length and 50 mm diameter. The hydraulic plunger is used to apply the pressure (100 MPa). The die temperature is 150 °C maintained constantly. The molten alloy was stirred at 250 rpm for 10 min [17] to achieve the homogeneous

dispersion. The reinforcement preheated in the furnace at 400 °C was introduced into the molten AA2024 slowly during stirring. In order to reduce the oxidation during the process, the experiments were conducted in an argon atmosphere. The molten alloy was poured into the die cavity and a squeeze pressure of 100 MPa was applied for 30 s by the punch. Die-metal interface promotes rapid heat transfer to solidify and then was ejected from the die. T4 condition was obtained by heat treating HMMC at 493 °C and then water quenched. Finally, aging was carried out at the room temperature. The samples were prepared according to ASTM standards to study the properties hardness, tensile strength, and wear.



**Fig. 1.** Squeeze casting machine setup

Structural and phase identification of the HMMCs were evaluated by using X-ray diffraction (XRD) analyzer using the model XRD-3000, SEI-FURT. XRD spectra were recorded with a graphite monochromatic Cu-K $\alpha$  radiation ( $\lambda = 1.5406 \text{ \AA}$ ) in the  $2\theta$  range from 5 to 70 ° with a scan rate of 2 °/min. The density of sample was determined using Archimedes principle on a Mettler Toledo ME204 apparatus (ASTM D792-91). Samples cut into small piece were weighed in air and water. Theoretical density was estimated by applying the rule of mixtures for different weight fraction of  $\text{Al}_2\text{O}_3/\text{SiC}$  particles. The difference between expected and observed density of the samples was used to evaluate the porosity.

Micro-hardness of HMMC samples was measured using the Vickers digital micro-hardness (Shimadzu JIS Q 17025) tester under the standard



Fig. 2. Specimen loaded on (Shimadzu) hardness tester



Fig. 3. Tensile and wear test samples

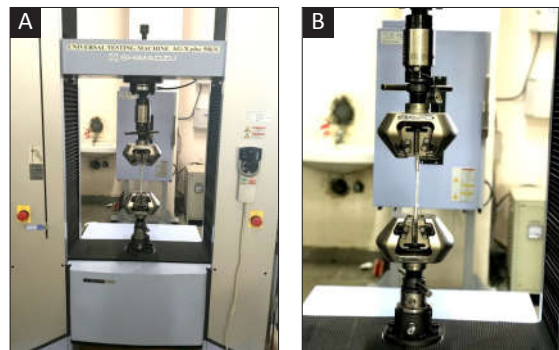


Fig. 4. Tensile Testing Machine (Shimadzu)  
a) Tensile testing machine  
b) Tensile test specimen loaded in the UTM

load of 0.05 Kg for the duration of 15 s (Fig. 2). For accurate measurements, the sample surfaces were ground and polished to create a well-defined indentation. To avoid the effect of segregation of particulates, the average of five tests was taken for each sample. The mechanical behavior of HMMCs was studied using the tensile test as per the standard ASTM E08-8. The composite sample with a diameter 6 mm and gauge length 30 mm was used for the tests being polished using 600 grit sand-paper before the measurements (Fig. 3). A computer-controlled tensile testing machine shown in Fig.4 (a) (Shimadzu JIS Q 17025) at a cross-head speed of  $0.5 \text{ mms}^{-1}$  was used for the tensile strength measurement. The tensile test sample loaded in the UTM is shown in Fig 4 (b).

Dry sliding wear behavior of HMMCs was investigated using the pin on a disc test system (DUCOM, TR-20LE); the samples were prepared as per the standard ASTM G99-05. Pin sample dimension selected was 6 mm in diameter and 15 mm in height, machined and polished metallographically as shown in Fig. 3. An oil hardened nickel steel (ONHS) of diameter 55 mm steel disc of 62 HRC was used as the counter surface in the wear test. Samples were tested at the ambient condition

where the relative humidity was about 60–65%. Wear test was performed at sliding speeds of 2, 3, 4 m/s for different loads of 10 and 20 N. The sliding distance and wear track diameter of 1200 m and 30 mm were used respectively. Measurements were performed in unlubricated condition. The weight loss of samples (cleaned with acetone) was determined by using an electronic weighing balance with a resolution of  $\pm 0.1 \text{ mg}$ . The coefficient of friction for the given sliding distance was recorded continuously. Wear-tested sample's surfaces and EDS analysis was done through scanning electron microscopy using the model CARL ZEISS SEM.

### 3. RESULTS AND DISCUSSION

#### 3.1. Phase Evolution of HMMCs

Fig.5 (a-f) shows the XRD pattern for  $\text{Al}_2\text{O}_3/\text{SiC}$  reinforced AA2024 metal matrix composite (10  $\mu\text{m}$  particle size). The XRD patterns indicate the presence of Al,  $\text{Al}_2\text{O}_3$ , SiC,  $\text{Al}_4\text{C}_3$  and  $\text{Al}_4\text{SiC}_4$  phases due to the reaction between Al and SiC particulates. The intensity of the peaks was found to vary with composition. It is clearly observed that the peak shift was observed with increasing wt%

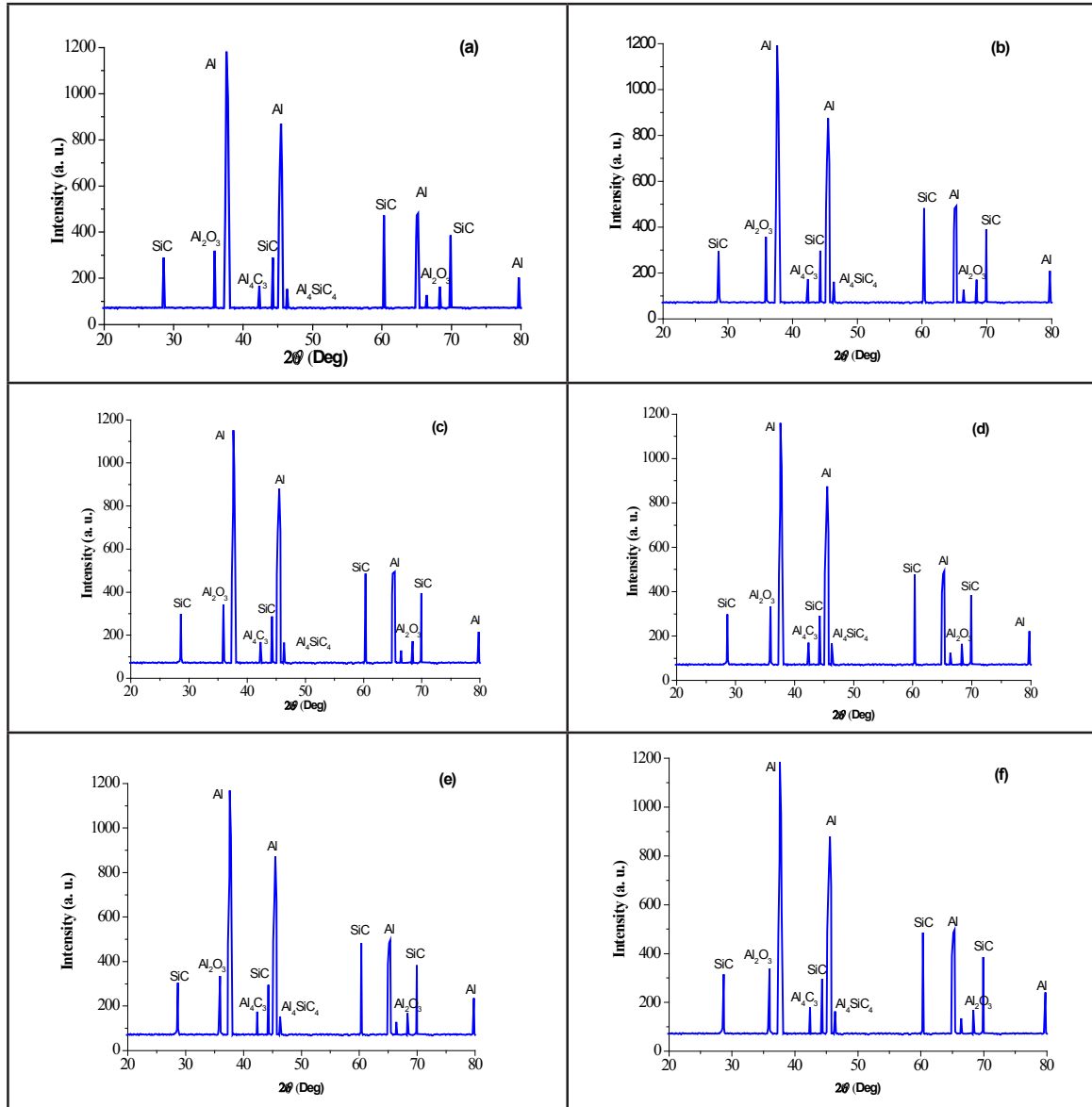


**Fig. 5.** XRD pattern for the samples (a) AA2024/0.5wt%Al<sub>2</sub>O<sub>3</sub>/0.5wt%SiC, (b) AA2024/1wt%Al<sub>2</sub>O<sub>3</sub>/1wt%SiC, (c) AA2024/2wt%Al<sub>2</sub>O<sub>3</sub>/2wt%SiC, (d) AA2024/3wt%Al<sub>2</sub>O<sub>3</sub>/3wt%SiC, (e) AA2024/4wt%Al<sub>2</sub>O<sub>3</sub>/4wt%SiC, and (f) AA2024/5wt%Al<sub>2</sub>O<sub>3</sub>/5wt%SiC.

of Al<sub>2</sub>O<sub>3</sub>/SiC reinforcements. (Fig 5. a-e). Fig. 5f indicates well-defined crystalline peaks. The peaks were compared with the standard diffraction data to analyze the presence of different phases. 2θ reflections at 37.60, 45.32, 65.13, 78.71 and 82.65 ° correspond to AA2024 phase. It exhibits FCC crystal structure with the lattice parameter of a = 0.404 nm which is comparable to the JCPDS No.85-1327. The Al<sub>2</sub>O<sub>3</sub> phase is confirmed from the peaks at 2θ, 35.81, 43.03, 68.32 and 66.42 ° that match with JCPDS card No.10-0173.

SiC peak at 2θ, 28.62, 44.18, 60.32 and 69.83 ° confirmed with the JCPDS No. 29-1128. The less intense peaks found at 2θ, 42.39 and 46.59 ° were due to the Al<sub>4</sub>C<sub>3</sub> and Al<sub>4</sub>SiC<sub>4</sub> that formed during the reaction at the interface between Al and SiC particulates [37-40]. However, no reaction is observed between the reinforcement Al<sub>2</sub>O<sub>3</sub> and the matrix Al. It is evidenced from the XRD pattern that the diffraction intensity and broadening of the peaks vary with volume fraction and particle size of reinforcement.

### 3.2. The density and Porosity of the Composites

The effect of different weight fraction and particle size of  $Al_2O_3/SiC$  reinforcement on the density and porosity of HMMCs is shown graphically in Figs. 6 and 7. The trend shows that the reinforcement weight fraction (1 to 10 wt%) and particle size play an important role in controlling the density of the composites. The composite density increased with increase in  $Al_2O_3/SiC$  reinforcement (up to 10 wt%) and particle size (Fig. 6). Furthermore, it is interesting to note that the HMMCs with 40  $\mu m$  particle size showed higher density than particle sizes with 20 and 10  $\mu m$ . The observed density is consistent with the results reported in the previous research [17, 41]. Fig. 7 shows the variation in porosities for different particle sizes and wt% of  $Al_2O_3/SiC$  reinforcement. The porosity was found to be high in the sample AA2024/0.5wt% $Al_2O_3$ /0.5wt%SiC. Porosity decreased with increasing wt% and particle size in the samples.

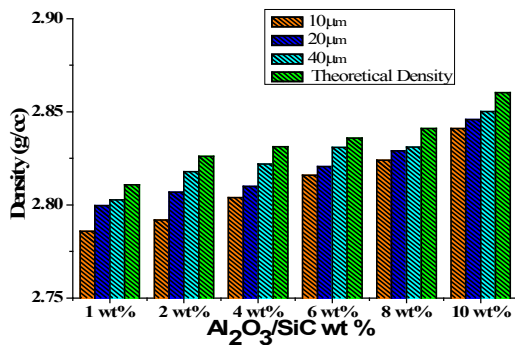


Fig. 6. The variation of density of the HMMCs with different weight fraction and particle size of  $Al_2O_3/SiC$  reinforcement.

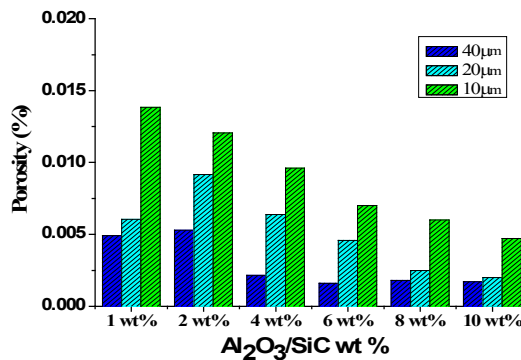


Fig. 7. The variation of porosity of the HMMCs with different weight fraction and particle size of  $Al_2O_3/SiC$  reinforcements

The observed densities were found to be a little low and closer to the theoretical density. Hence porosities were unavoidable in all the samples. It seems porosity in MMCs is unavoidable to some extent due to the steps involved in the fabrication process. The creation of air bubbles during the stirring, air contact with molten metal during pouring, the evolution of hydrogen and shrinkage during the solidification are reasons for the porosity [17, 42]. Observation shows that the porosity in the composite sample showed the highest for 40  $\mu m$  particle size in all of the samples with the increasing wt% of  $Al_2O_3/SiC$  reinforcement. The major reason is the squeeze pressure that applied with better wettability that provided the strong bonding force between AA2024 and  $Al_2O_3/SiC$  reinforcement.

### 3.3. Mechanical Properties of the Composites

#### 3.3.1. Vickers Hardness Test

Fig. 8 shows the Vickers hardness of AA2024/ $Al_2O_3/SiC$  hybrid composites. HMMC hardness increased with the increase in reinforcement wt% and decreasing particle size. The different weight fractions of  $Al_2O_3/SiC$  reinforcement significantly improve the hardness of the metal matrix as observed in various reports [43-45]. It is also noticed from the results the particle size of the reinforcement influences the hardness of the HMMC. The composite samples fabricated with the reinforcement particle size of 10  $\mu m$ , showed the highest hardness compared to the hardness of particle sizes of 20 and 40  $\mu m$ . HMMC sample

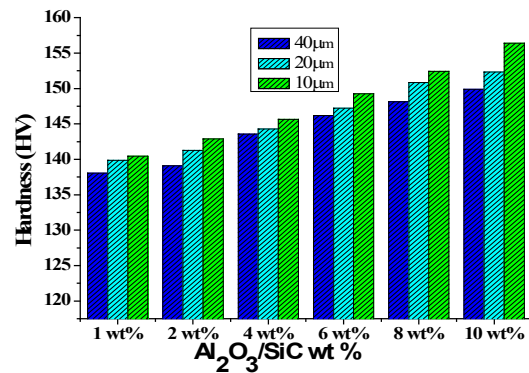


Fig. 8. The variation of Vickers hardness with different fraction of  $Al_2O_3/SiC$  reinforcements and particle sizes

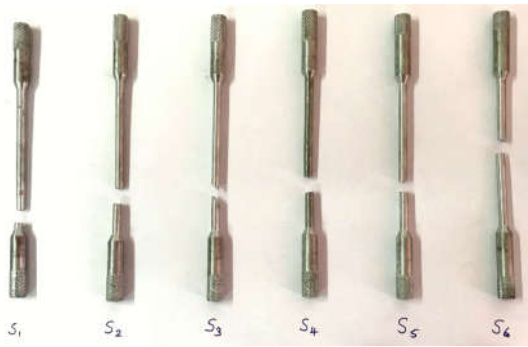


Fig. 9. HMMCs reinforced with 10  $\mu\text{m}$  particle size subjected to tensile strength test

AA2024/5wt%Al<sub>2</sub>O<sub>3</sub>/5wt%SiC with the particle size of 10  $\mu\text{m}$  revealed the highest hardness 156.4 HV. Higher the weight fraction of Al<sub>2</sub>O<sub>3</sub>/SiC, harder and well-bonded particulates in metal matrix increases the constraint to the plastic deformation and dislocation density increases the hardness of HMMCs [46]. Therefore, the experimental results conclude that the addition of hard Al<sub>2</sub>O<sub>3</sub>/SiC reinforcement improved the hardness of the AA2024 alloy by 14.1 %.

### 3.3.2. Tensile Strength

HMMCs sample fabricated with 10  $\mu\text{m}$  subjected to tensile strength test is shown in Fig. 9. Tensile strength of HMMCs showed the trend similar to the hardness that varied with different weight fraction of reinforcement and particle sizes (Fig.10). The sample (AA2024/5wt%Al<sub>2</sub>O<sub>3</sub>/5wt%SiC) with 10  $\mu\text{m}$  reinforced particle size showed the maximum tensile strength that was found to be 531.43 MPa [31]. Tensile strength of the composite increased with increase in Al<sub>2</sub>O<sub>3</sub>/SiC reinforcement up to 10 wt% and a decrease in particle size from 40 to 10  $\mu\text{m}$ . The particle size and wt% of the reinforcement play a significant role in increasing the tensile strength of composites.

Hard Al<sub>2</sub>O<sub>3</sub>/SiC reinforcement strongly bonded to the AA2024 matrix is responsible for the increase in dislocation density near the matrix-reinforcement interface and grain strengthening effect [47, 48]. The dislocation density increase is mainly due to the increase in wt% of SiC that hinders the dislocation motion [49]. Tensile strength of the HMMCs is 13.3 % higher than AA2024 metal

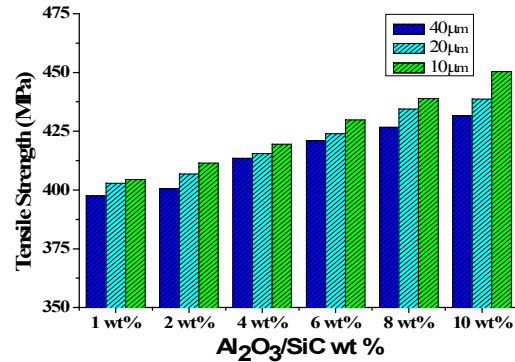


Fig. 10. The variation of tensile strength with Al<sub>2</sub>O<sub>3</sub>/SiC particle content and size.

matrix and was found to be substantial [40, 50]. It is evident that the reinforcement with 10  $\mu\text{m}$  particle size having strong interfacial bonding between the AA2024 alloy and Al<sub>2</sub>O<sub>3</sub>/SiC particulates enhanced the tensile strength. Tensile strength of the HMMCs is 13.3 % higher than that of AA2024 metal matrix.

Generally, the ductility of Al alloy based composites is quantified by tensile elongation. For the composite sample, AA2024/5wt%Al<sub>2</sub>O<sub>3</sub>/5wt%SiC with 10  $\mu\text{m}$  particle size, elongation measured was 4 % lower than AA2024 (6 %). Tensile elongation was found to be high for the composite sample with 20 and 40  $\mu\text{m}$  particle sizes. Composite sample AA2024/0.5wt%Al<sub>2</sub>O<sub>3</sub>/0.5wt%SiC showed the highest elongation. Further elongation decrease with increasing wt% of Al<sub>2</sub>O<sub>3</sub>/SiC [17, 50-52]. Though the addition of reinforcement contributes to an increase in hardness and tensile strength, it showed a decrease in elongation percentage. The results of this research were consistent with the previous literature [53]. This considerable decrease in ductility is due to the addition of reinforcement.

### 3.4. Wear Properties of the Composites

HMMC generally possesses high specific strength and superior wear resistance. Addition of ceramic particles into the metal matrix improves the seizure resistance compared to the pure alloy. It is reported that AA2024 reinforced with Al<sub>2</sub>O<sub>3</sub>/SiC and graphite particulates with 10 $\mu\text{m}$  particle size exhibit better mechanical properties [16, 29, 36]. Hence, HMMC with 10 $\mu\text{m}$  reinforcement

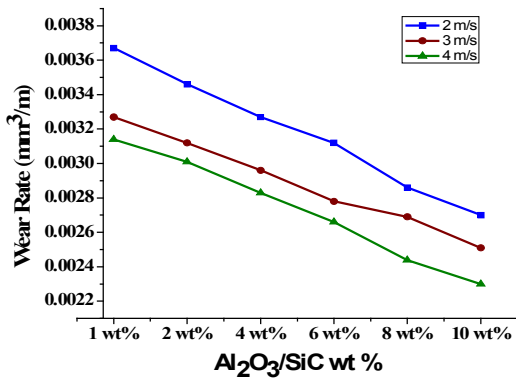


Fig. 11. The wear rate for HMMC (10 μm particle Size) with varying sliding speeds at load 10N.

particle size was selected for wear study. Fig. 11 shows the dry sliding wear behavior of composites at three different velocities 2, 3 and 4 m/s. A decrease in wear rate was observed with the increase in reinforcement wt% at different velocities. The wear rate was found to be the lowest for the sample (AA2024/5wt%Al<sub>2</sub>O<sub>3</sub>/5wt%SiC) tested at the constant velocity of 4 m/s.

The sample (AA2024/0.5wt%Al<sub>2</sub>O<sub>3</sub>/0.5wt%SiC) wear rate was found to be higher than others for the different velocities at 10 N loads. During the wear test process, SiC reinforcement thrown out of the composite pin gets logged on the disk. This converts the adhesive wear into abrasive wear. Due to this reason, a greater amount of material is removed from the pin sample with lower wt% of reinforcement (AA2024/0.5wt%Al<sub>2</sub>O<sub>3</sub>/0.5wt%SiC). The composite wear loss decreased with the increase in velocity and reinforcement wt% of HMMCs (Fig. 11). The main reason is the dispersion of reinforcement act as

load bearing components [54]. The other reason being the increase in interfacial temperature that creates the oxidation layer on the composite. The oxide layer acted as a protective layer that prevents sliding interfaces [55]. Hence, increasing the sliding velocity increased the thickness of the protective layer over the entire surface of the pin, thus resulting in less wear loss. Increase in sliding velocity from 2 to 4 m/s, decreased the composite wear rate by 37.3 %.

The variation in wear rate at various loads for the constant sliding velocity 4m/s for 10μm particle size is shown in Fig. 12. A decrease in wear was observed with an increase in reinforcement from 1 to 10 wt% for Al<sub>2</sub>O<sub>3</sub>/SiC, respectively. With the increase in wt% of the reinforcement, SiC in the composite increased the contact area with the steel counterface that improved the wear resistance. The wear rate (Fig. 12) increased with increase in load due to the increased frictional forces that lead to high coefficient of friction at low wt% (1-6 wt%) of Al<sub>2</sub>O<sub>3</sub>/SiC. In addition, the frictional force increases the temperature of the composite which in turn increased the wear rate during the sliding process [56]. The decrease in wear rate was observed from 0.00307 to 0.00221 for 10 N and 0.00314 to 0.00225 for 20 N, respectively. The wear resistance improved by 29.6 %. The increase in reinforcement wt% and load from 10 to 20 N increased the wear rate.

Fig. 13 shows the effect of friction coefficient of HMMCs with 10 μm particle size at different loads. It showed a decreasing trend with an increase in wt% of reinforcement at constant load. However, the coefficient of friction was found to

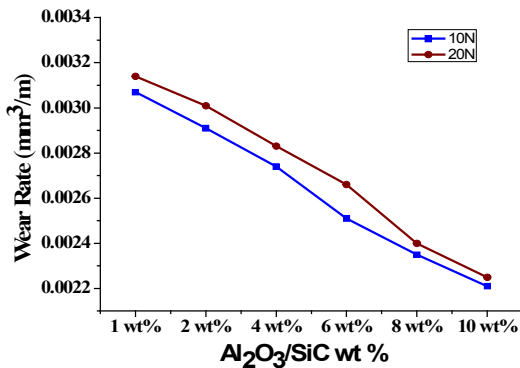


Fig. 12. The wear rate of HMMC (10 μm particle Size) with varying loads

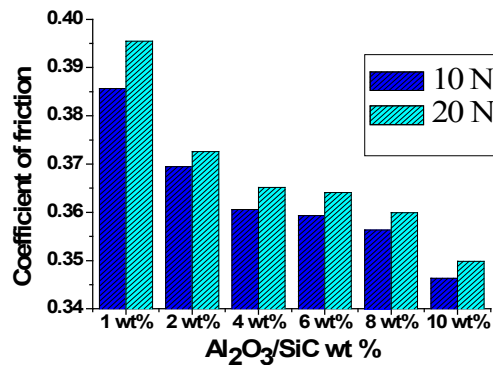


Fig. 13. Coefficient of friction of HMMC (10 μm particle Size) with varying loads



be high at the 20 N load. It is known that the interaction between the load and the sliding distance demonstrated a significant effect on the wear behavior of the composites [57]. Presence of hard reinforcement  $\text{Al}_2\text{O}_3$  confirmed the role of solid lubricant [58]. Interaction of  $\text{Al}_2\text{O}_3$  particles on the wear surface prevents the metal-metal surface contact that reduced the coefficient of friction between the pin and the disk. The coefficient of friction decreased from 0.385 to 0.346 for 10 N and for the 20 N load from 0.395 to 0.349, respectively. The results revealed that the coefficient of friction decreased by 12.4 % with a decrease in load from 10 to 20 N. Increased wear resistance

with decreased coefficient of friction is due to the presence of protective layer over the entire surface of the pin as confirmed in the previous literature showing that the  $\text{Al}_2\text{O}_3$  and  $\text{B}_4\text{N}$  particles act as solid lubricant [54,58]. The results convey that frictional behavior of the HMMCs depends on load, sliding speed and reinforcement wt%.

### 3.5. Morphological Analysis

Fig.14 illustrates the micrograph of typical AA2024/ $\text{Al}_2\text{O}_3$ /SiC composites with 10 $\mu\text{m}$  particle size exposed to the 20 N loads. SEM micrographs revealed that the HMMCs show both

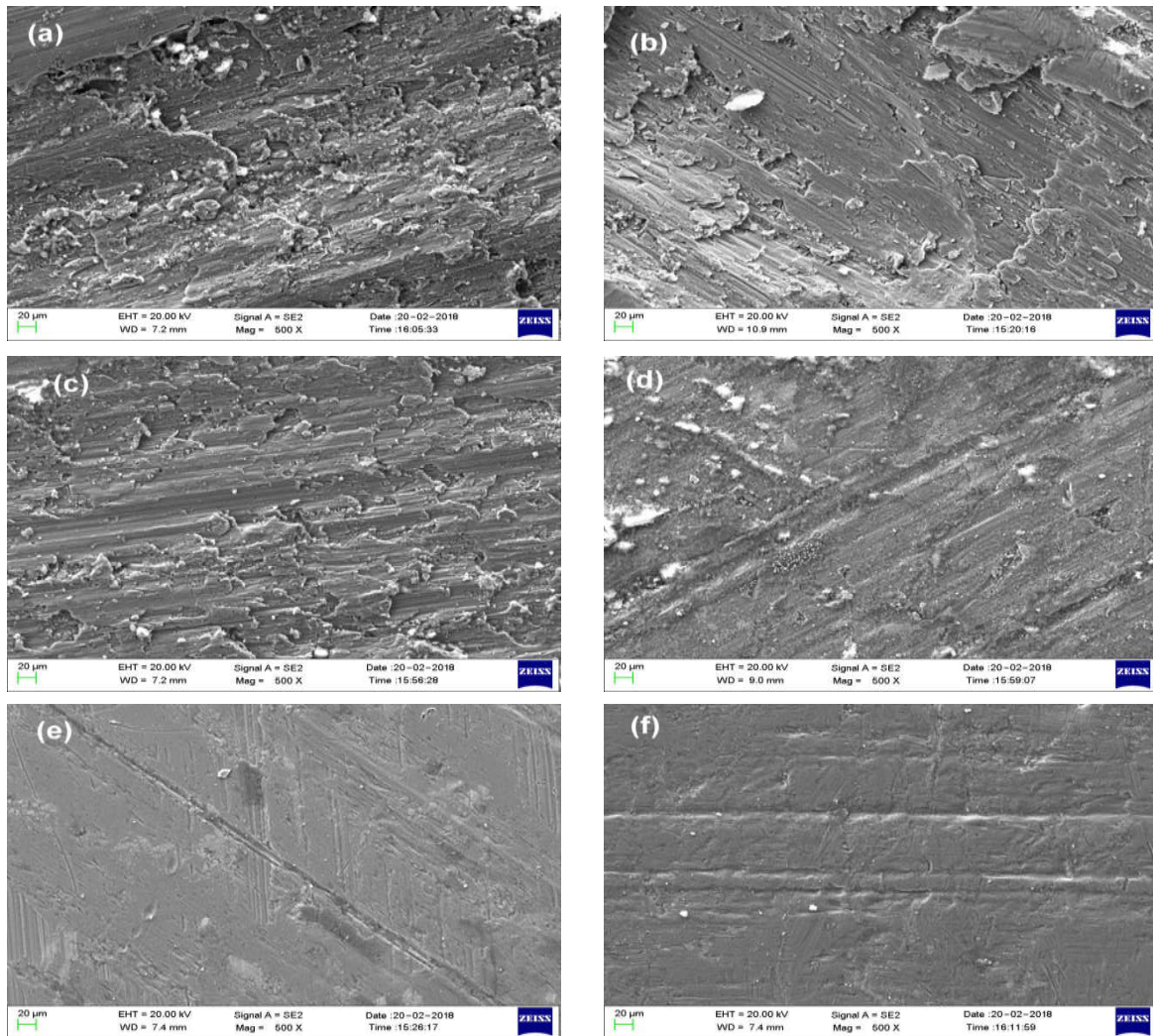


**Fig. 14.** SEM micrograph of the worn surfaces of HMMC samples (a) AA2024/0.5wt% $\text{Al}_2\text{O}_3$ /0.5wt%SiC, (b) AA2024/1wt% $\text{Al}_2\text{O}_3$ /1wt%SiC, (c) AA2024/2wt% $\text{Al}_2\text{O}_3$ /2wt%SiC, (d) AA2024/3wt% $\text{Al}_2\text{O}_3$ /3wt%SiC, (e) AA2024/4wt% $\text{Al}_2\text{O}_3$ /4wt%SiC, and (f) AA2024/5wt% $\text{Al}_2\text{O}_3$ /5wt%SiC, at load 20 N.

abrasive and adhesive wear along the wear track sliding direction. Also, some loose debris particles were observed on the surface of the composites and a thin film is formed between the two contacting surfaces. The microstructural analysis gave a clear distinction about the mechanism of material removal at higher loads exhibited adhesive wear. Micrograph 14 (a-c) showed severely damaged regions indicates the patches and abrasion in the worn surface [57, 58]. It shows the presence of  $Al_2O_3/SiC$  particles with cracks inside the worn path. Fig 15 shows the EDS analysis for the sample AA2024/0.5wt% $Al_2O_3$ /0.5wt%SiC which exhibit different chemical composition being rich in Al and other elements such as Si, C, Mg, O, and Fe. The results of EDS analysis are summarized in Table 2. The composite contains about 87.35 wt% Al, 8.41 wt% of C and 2.15 wt% O. Illustration from Fig. 14 (c,d) shows cavities and grooves along the slide direction in the samples AA2024/2wt% $Al_2O_3$ /2wt%SiC and AA2024/3wt% $Al_2O_3$ /3wt%SiC. The reinforcement removed forms a thin tribo film that prevents the direct contact between the metal and the sliding

surface preventing the breaking of  $Al_2O_3$  particles. Hence, the wear rate observed is low compared to the sample AA2024/0.5wt% $Al_2O_3$ /0.5wt%SiC. The reinforcement  $Al_2O_3/SiC$  acted as a protective layer. From the Fig 14 (e) small patches were observed in the sample AA2024/4wt% $Al_2O_3$ /4wt%SiC, as  $Al_2O_3/SiC$  reinforcement acted as a barrier preventing the movement of dislocation. It is observed that small fragments of the material have been removed inside and on the edges of the wear track. Sample AA2024/5wt% $Al_2O_3$ /5wt%SiC with small cracks inside the worn path represented a smoother surface than other samples (Fig. 14 f). It demonstrated that the composite sample AA2024/5wt% $Al_2O_3$ /5wt%SiC showed better deformation resistance and wear. This resulted in decreased material removal rate during the wear test. The presence of  $Al_2O_3/SiC$  also noticed on HMMC worn surfaces with the EDS analysis is shown in Fig. 16. The corresponding chemical composition of EDS results is presented in table 3.

It is interesting to note that in this wear study, deformation resistance offered by SiC, fractured into small pieces that produced wear debris parti-

**Table 2.** Results of EDS measurements of AA2024/0.5wt% $Al_2O_3$ /0.5wt%SiC hybrid metal matrix

Element	Weight%	Atomic%
C K	8.41	16.93
O K	2.15	3.25
Mg K	0.90	0.89
Al K	87.35	78.23
Si K	0.44	0.38
Fe L	0.75	0.32
Totals	100.00	

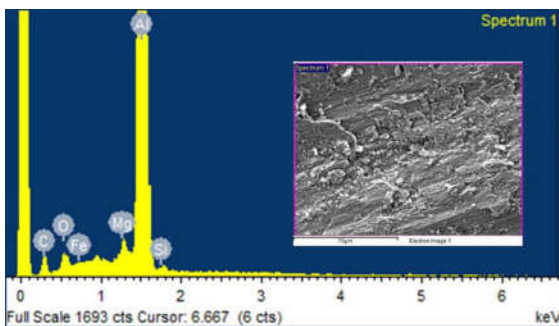


**Fig.15.** EDS analysis for the sample AA2024/0.5wt% $Al_2O_3$ /0.5wt%SiC

**Table 3.** Results of EDS measurements of AA2024/5wt% $Al_2O_3$ /5wt%SiC hybrid metal matrix

Element	Weight%	Atomic%
C K	4.12	8.05
O K	30.08	44.09
Mg K	0.27	0.26
Al K	44.16	38.38
Si K	0.38	0.32
Cr L	2.56	1.15
Fe L	18.42	7.74
Totals	100.00	

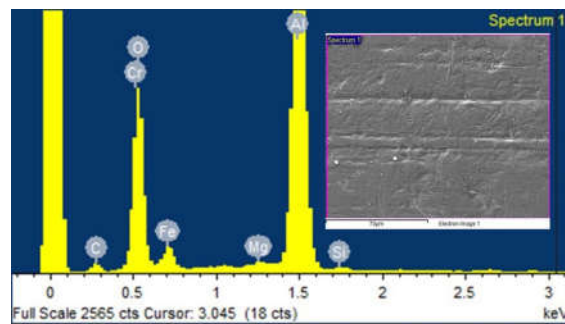


**Fig. 16.** EDS analysis for the sample AA2024/5wt% $Al_2O_3$ /5wt%SiC

cle. This debris prevents the disk from penetrating into the metal protecting the soft aluminum matrix, thereby increasing the wear resistance.

#### 4. CONCLUSIONS

HMMCs with different weight percentages and particle sizes of  $\text{Al}_2\text{O}_3/\text{SiC}$  reinforcement were successfully prepared by squeeze casting method. The samples were characterized and drawn the following conclusions:

1. Composite density increased with increasing weight percentage and decreasing particles size of  $\text{Al}_2\text{O}_3/\text{SiC}$  reinforcement.
2. AA2024/5wt% $\text{Al}_2\text{O}_3$ /5wt%SiC (10 $\mu\text{m}$  particle size) showed maximum hardness and tensile strength of 156.4 HV and 531.43 MPa, respectively.
3. Wear study revealed that the most important factor affecting the friction coefficient of the hybrid composite is the load followed by sliding speed. The decrease in wear rate was observed from 0.00307 to 0.00221 for 10 N and 0.00314 to 0.00225 for 20 N, respectively.
4. The coefficient of friction decreased from 0.385 to 0.346 for 10 N and for the 20 N load from 0.395 to 0.349, respectively.

The results derived from this research claims that  $\text{Al}_2\text{O}_3/\text{SiC}$  (10  $\mu\text{m}$  particle size) reinforced AA2024 significantly enhanced the mechanical and wear properties. Therefore, it can be concluded that prepared HMMCs stands as the best-suited material with characteristics in the application of engine cylinder liner to meet the modern demands of the automotive industries.

#### 5. ACKNOWLEDGMENT

Authors would like to acknowledge the Management and Dean-SMBS, VIT, Chennai, India for providing the necessary support to carry out this research. Our special thanks to Bio-technology division, VIT, Vellore for the permission rendered to carry out the EDS analysis. Our sincere thanks to Strength materials laboratory, VIT, Chennai for providing the Tensile and Hardness test facility to pursue this research.

#### REFERENCE

1. Stojanović, B. and Lozica Ivanović, "Application of aluminium hybrid composites in automotive industry". *Tehnički vjesnik*, 2015, 22, 247-251.
2. Mortensen, A. and Llorca, J., "Metal matrix composites." *Annu. Rev. Mater. Res.*, 2010, 40, 243-270.
3. Surappa, M. K., "Aluminium matrix composites: Challenges and opportunities." *Sadhana*, 2003, 28, 319-334.
4. Kim, S. J., Kim, K. S. and Jang, H., "Optimization of manufacturing parameters for a brake lining using Taguchi method." *J. Mater. Process. Tech.*, 2003, 136, 202-208.
5. Poddar, Palash, et al., "Processing and mechanical properties of SiC reinforced cast magnesium matrix composites by stir casting process." *Mater. Sci. Eng. A*, 2007, 460: 357-364.
6. Prasad, S. V. and Asthana, R., "Aluminum metal-matrix composites for automotive applications: tribological considerations." *Tribol. Lett.*, 2004, 17, 445-453.
7. Basavarajappa, S., Chandramohan, G. and Davim, J. P., "Application of Taguchi techniques to study dry sliding wear behaviour of metal matrix composites." *Mater. Des.*, 2007, 28, 1393-1398.
8. Ozden, S., Ekici, R. and Nair, F., "Investigation of impact behaviour of aluminium based SiC particle reinforced metal-matrix composites." *Compos. Part A Appl. Sci. Manuf.*, 2007, 38, 484-494.
9. Kaczmar, J. W., Pietrzak, K. and Włosiński, W., "The production and application of metal matrix composite materials." *J. Mater. Process. Tech.*, 2000, 106, 58-67.
10. Onat, A., Akbulut, H. and Yilmaz, F., "Production and characterisation of silicon carbide particulate reinforced aluminium-copper alloy matrix composites by direct squeeze casting method." *J. Alloys. Compd.*, 2007, 436, 375-382.
11. Natrayan, L., Kumar, M. S. and Palanikumar, K., "Optimization of squeeze cast process parameters on mechanical properties of  $\text{Al}_2\text{O}_3/\text{SiC}$  reinforced hybrid metal matrix composites using taguchi technique." *Mater Res Express*, 2018, 5, 066516.
12. Law, E., Dai Pang, S. and Quek, S. T., "Discrete dislocation analysis of the mechanical response of silicon carbide reinforced aluminum nano composites. *Compos Part B-Eng.*," 2011, 42, 92-98.
13. Senthilkumar, V. and Omprakash, B. U., "Effect of Titanium Carbide particle addition in the aluminium composite on EDM process parameters." *J. Manuf. Process.*, 2011, 13, 60-66.
14. Murty, S. N., Rao, B. N. and Kashyap, B. P., "On

- the hot working characteristics of 6061Al–SiC and 6061–Al<sub>2</sub>O<sub>3</sub> particulate reinforced metal matrix composites.” *Composites sci. technol.*, 2003, 63(1), 119-135.
15. Natrayan, L., Singh, M. and Kumar, M. S., “An experimental investigation on mechanical behaviour of SiCp reinforced Al 6061 MMC using squeeze casting process.” *Inter J Mech Prod Engi Res Develop.*, 2017, 7, 663-668.
  16. Abdel-Azim, A. N., Shash, Y., Mostafa, S. F. and Younan, A., “Casting of 2024-Al alloy reinforced with Al<sub>2</sub>O<sub>3</sub> particles.” *J. Mater. Process. Tech.*, 1995, 55, 199-205.
  17. Kok, M., “Production and mechanical properties of Al<sub>2</sub>O<sub>3</sub> particle-reinforced 2024 aluminium alloy composites *J. Mater.*” *Process. Tech.*, 2005, 161, 381-387.
  18. K k, M. and  zdin, K., “Wear resistance of aluminium alloy and its composites reinforced by Al<sub>2</sub>O<sub>3</sub> particles. *J. Mater. Process.*” *Tech.*, 2007, 183, 301-309.
  19. Hajjari, E. and Divandari, M., “An investigation on the microstructure and tensile properties of direct squeeze cast and gravity die cast 2024 wrought Al alloy.” *Mater. Des.*, 2008, 29, 1685-1689.
  20. Balasivanandha, Prabu, S., “Influence of stirring speed and stirring time on distribution of particles in cast metal matrix composite.” *J. Mater. Process. Tech.*, 2006, 171, 268-273.
  21. Basavarajappa, S., Chandramohan, G. and Dinesh, A., “Mechanical properties of mmc’s-An experimental investigation”. In *Int. symposium of research on Materials and Engineering*, IIT- Madras, 2004, 20, 1-8.
  22. Rao, R. N. and Das, S., “Effect of matrix alloy and influence of SiC particle on the sliding wear characteristics of aluminium alloy composites.” *Mater. Des.*, 2010, 31, 1200-1207.
  23. Miracle, D. B., “Metal matrix composites—from science to technological significance. *Compos.*” *Sci. Technol.*, 2005, 65, 2526-2540.
  24. Sahin, Y. and Murphy, S., “The effect of fibre orientation of the dry sliding wear of borsic-reinforced 2014 aluminium alloy. *J. Mater.*” *Sci.*, 1996, 31, 5399-5407.
  25. Kok, M., “Production and mechanical properties of Al<sub>2</sub>O<sub>3</sub> particle-reinforced 2024 aluminium alloy composites.” *J. Mater. Process. Tech.*, 2005, 161, 381-387.
  26. Hashim, J., Looney, L. and Hashmi, M. S. J., “Particle distribution in cast metal matrix composites-Part I. *J. Mater.*” *Process. Tech.*, 2002, 123, 251-257.
  27. Zhong, Y., Guoyue, S. U. and Ke, Y. A. N. G., “Micro segregation and improved methods of squeeze casting 2024 aluminium alloy.” *J. Mater. Sci. Tech.*, 2009, 19, 413-416.
  28. Yoshie, N., “Effect of flux dispersion behavior on desulfurization of hot metal.” *ISIJ international*, 2010, 50, 403-410.
  29. Shiming, H., “Effect of consolidation parameters and heat treatment on microstructures and mechanical properties of SiCp/2024 Al composites. *Sci.*” *Eng. Compos. Mater.*, 2015, 22, 673-684.
  30. Zhang, X. N., Geng, L. and Wang, G. S., “Fabrication of Al-based hybrid composites reinforced with SiC whiskers and SiC nanoparticles by squeeze casting.” *J. Mater. Process. Tech.*, 2006, 176, 146-151.
  31. Myriounis, D. P., “Effects of heat treatment on microstructure and the fracture toughness of SiCp/Al alloy metal matrix composites.” *Journal of advanced materials*, 2009, 41, 18-27.
  32. Yigezu, B. S., Jha, P. K. and Mahapatra, M. M., “The key attributes of synthesizing ceramic particulate reinforced Al-based matrix composites through stir casting process: A review.” *Mater. Manuf. Process.*, 2013, 28, 969-979.
  33. Chatterjee, S., Ghosh Sur, S., Bandyopadhyay, S. and Basumallick, A., “Effect of microstructure and residual stresses on nano-tribological and tensile properties of Al<sub>2</sub>O<sub>3</sub>-and SiC-reinforced 6061-Al metal matrix composites.” *J. Compos Mater.*, 2016, 50, 2687-2698.
  34. Venkatesan, S. and Xavier, M. A., “Analysis of Mechanical Properties of Aluminum Alloy Metal Matrix Composite by Squeeze Casting—A Review”. *Materials Today: Proceedings*, 2018, 5, 11175-11184.
  35. Vijayaram, T. R., et al., “Fabrication of fiber reinforced metal matrix composites by squeeze casting technology.” *J. Mater. Sci. Technol.*, 2006, 178, 34-38.
  36. Leng, Jinfeng, et al., “Mechanical properties of SiC/Gr/Al composites fabricated by squeeze casting technology.” *Scr. Mater.*, 2008, 59, 619-622.
  37. Tham, L. M., Gupta, M. and Cheng, L., “Effect of limited matrix–reinforcement interfacial reaction on enhancing the mechanical properties of aluminium–silicon carbide composites. *Acta Mater.*,” 2001, 49, 3243-3253.
  38. Boopathi, M. M., Arulshri, K. P. and Iyandurai, N., “Evaluation of mechanical properties of aluminium alloy 2024 reinforced with silicon carbide and fly ash hybrid metal matrix composites.” *Am. J. Appl. Sci.*, 2013, 10, 219.
  39. Kiourtsidis, G. E. and Skolianos, S. M., “Wear

- behavior of artificially aged AA2024/40  $\mu\text{m}$  SiCp composites in comparison with conventionally wear resistant ferrous materials". *Wear*, 2002, 253, 946-956.
40. Shorowordi, K., "Microstructure and interface characteristics of B4C, SiC and  $\text{Al}_2\text{O}_3$  reinforced Al matrix composites: a comparative study." *J. Mater. Process. Tech.*, 2003, 142, 738-743.
  41. Sahin, Y., "Preparation and some properties of SiC particle reinforced aluminium alloy composites." *Mater. Des.*, 2003, 24, 671-679.
  42. Madsen, B. and Lillholt, H., "Physical and mechanical properties of unidirectional plant fibre composites-an evaluation of the influence of porosity." *Compos. Sci. Technol.*, 2003, 63, 1265-1272.
  43. Thakur, S. K. and Dhindaw, B. K., "The influence of interfacial characteristics between SiCp and Mg/Al metal matrix on wear coefficient of friction and micro hardness. *Wear*," 2001, 247, 191-201.
  44. Suresha, S. and Sridhara, B. K., "Effect of addition of graphite particulates on the wear behaviour in aluminium-silicon carbide-graphite composites." *Mater. Des.*, 2010, 31, 1804-1812.
  45. Natrayan, L. and M. Senthil Kumar., "Study on Squeeze Casting of Aluminum Matrix Composites-A Review." *Advanced Manufacturing and Materials Science*. Springer, Cham, 2018, 75-83.
  46. Manoj, S., "Development of aluminium based silicon carbide particulate metal matrix composite." *Journal of Minerals and Materials Characterization and Engineering*, 2009, 8, 455.
  47. Karthigeyan, R., Ranganath, G. and Sankaranarayanan, S., "Mechanical properties and microstructure studies of aluminium (7075) alloy matrix composite reinforced with short basalt fibre. *Eur. J. Sci. Res.*, 2012, 68, 606-615.
  48. Kumar, M. S., "Experimental investigations on mechanical and microstructural properties of  $\text{Al}_2\text{O}_3/\text{SiC}$  reinforced hybrid metal matrix composite." *IOP Conf Ser Mater Sci Eng.*, 2018, 402, 012123.
  49. Radhika, N. and Subramaniam, R., "Wear behaviour of aluminium/alumina/graphite hybrid metal matrix composites using Taguchi's techniques." *Ind. Lubr. Tribol.*, 2013, 65, 166-174.
  50. Umanath, K., Palanikumar, K. and Selvamani, S. T., "Analysis of dry sliding wear behaviour of Al6061/SiC/ $\text{Al}_2\text{O}_3$  hybrid metal matrix composites. *Compos Part B-Eng.*" 2013, 53, 159-168.
  51. Yigezu, B. S., Mahapatra, M. M. and Jha, P. K., "Influence of reinforcement type on microstructure, hardness, and tensile properties of an aluminum alloy metal matrix composite." *Journal of Minerals and Materials Characterization and Engineering*, 2013, 1, 124.
  52. Tian, J. and Shobu, K., "Fracture strength of melt-infiltrated SiC-mullite composite." *J. Mater. Sci.*, 2004, 39, 3751-3755.
  53. Rahman, M. H. and Al Rashed, H. M., "Characterization of silicon carbide reinforced aluminum matrix composites". *Procedia Engineering*, 2014, 90, 103-109.
  54. Ahmadi, A., Toroghinejad, M. R. and Najafizadeh, A., "Evaluation of microstructure and mechanical properties of Al/ $\text{Al}_2\text{O}_3$ /SiC hybrid composite fabricated by accumulative roll bonding process." *Mater.Des.*, 2014, 53, 13-19.
  55. Surappa, M. K., "Synthesis of fly ash particle reinforced A356 Al composites and their characterization." *Mater. Sci. Eng. A*, 2008, 480, 117-124.
  56. Altinkok, N., Özsert, I. and Findik, F., "Dry Sliding Wear Behavior of  $\text{Al}_2\text{O}_3/\text{SiC}$  Particle Reinforced Aluminium Based MMCs Fabricated by Stir Casting Method. *Acta Phys.*" *Pol.A.*, 2013, 124, 11-19.
  57. Sahin, Y. and Özdin, K., "A model for the abrasive wear behaviour of aluminium based composites. *Mater. Des.*, 2008, 29, 728-733.
  58. Arulraj, M. and Palani, P. K., "Parametric optimization for improving impact strength of squeeze cast of hybrid metal matrix (LM24-SiC p-cocunut shell ash) composite." *J Braz Soc Mech Sci.*, 2018, 40, 2.